Adult cortical plasticity depends on an early postnatal critical period.

by

Stuart D. Greenhill[1*], *Konrad Juczewski*[2*], *Annelies M. de Haan*[1], *Gillian Seaton*[1], *Kevin Fox*[1] *and Neil R. Hardingham*[1]

*joint first authors.

[1]School of Biosciences, Cardiff University

and

[2]NIAAA, NIH, Rockville

Development of the cerebral cortex is influenced by sensory experience during distinct phases of postnatal development known as critical periods. Disruption of experience during a critical period produces neurons that lack specificity for particular stimulus features, such as location in the somatosensory system. Synaptic plasticity is the agent by which sensory experience affects cortical development. Here we describe, in mice, a developmental critical period that affects plasticity itself. Transient neonatal disruption of signaling via the C-terminal domain of *disrupted in schizophrenia-1* (DISC1), a molecule implicated in psychiatric disorders, resulted in a lack of LTP and experience-dependent potentiation in adulthood. LTD and reversal of LTD were present though impaired in adolescence and absent in adulthood. These changes may form the basis for the cognitive deficits associated with mutations in DISC1 and the delayed onset of a range of psychiatric symptoms in late adolescence.

Disrupted in schizophrenia 1 (DISC1) is a protein that when mutated predisposes the human carrier for a number of mental disorders including schizophrenia, bipolar disorder, recurrent major depression and autism(1,2). DISC1 interacts with a surprisingly large number of signaling molecules including phosphodiesterase 4, Glycogen synthase kinase 3, Kalirin7, Fasciculation and elongation protein zeta 1, Kendrin, Lissencephaly 1 (Lis1) and Neurodevelopment Protein 1-Like 1 (Nudel)(3-8). DISC1 affects diverse aspects of neuronal development such as proliferation, migration and neurite extension. In addition, DISC1 is known to be expressed in cortical neurons both during development and during adulthood(9) and to reside at the post-synaptic density (6,10-12), though very little is understood of the role it plays there. In this study, working with mice, we asked whether DISC1 protein-protein interactions early in development are critical for synaptic plasticity in adulthood. We disrupted transiently DISC1's interaction with Lis1 and Nudel during early development, at a time after cortical neurogenesis and cell migration (which are complete by about postnatal day 7 in the mouse) but before synaptogenesis and dendrite formation dominate.

We studied adult plasticity in the mouse barrel cortex, a primary sensory cortical area that receives tactile information from a normal array of 40 large whiskers. We removed all but one whisker on one side of the face of adult mice (13) to invoke cortical plasticity. The single-whisker experience normally leads to expansion of the cortical territory responding to the spared whisker (Figure 1A). To manipulate DISC1 interactions with Lis1 and Nudel, we used a conditional transgenic mouse expressing the DISC1 C-terminal domain (DISC1cc; residues 671-852), which interacts with Lis1 and Nudel (14-16) in a tamoxifen sensitive construct. Within this system, a single tamoxifen injection affects DISC1 signaling for 6-48 hours (P7-P9) (15). Spatial expression of DISC1cc is restricted to excitatory neurons in the forebrain by the αCaMKII promoter and its activity is controlled by tamoxifen. We studied the effect of a single subcutaneous injection of tamoxifen at P7 on single-whisker plasticity in adulthood (age range P70 - 130).

We found that adult DISC1cc mice injected with tamoxifen at P7 and with whiskers intact, developed a normal barrel pattern, and normal cortical layers, cell density and receptive fields (Figure S1). However, experience-dependent potentiation invoked by whisker loss was absent in DISC1cc mice injected with tamoxifen [$F_{(7,51)}$=6.9, $p<0.001$, 3-way ANOVA, see Figure 1]. Plasticity in cortical layers 2 and 3 (L2/3) was normal in wild-type mice receiving tamoxifen, indicating that tamoxifen only acted via the mutant protein and not by perturbing estrogen signaling ($t_{(11)}$=2.9, $p<0.02$). Plasticity was also normal in DISC1cc mice given just vehicle at P7, indicating that background levels of DISC1cc availability are effectively zero (Figure 1; $t_{(11)}$=2.4, $p<0.05$; NB: the mutated ligand binding domain fused to DISC1cc does not bind natural estrogen, only tamoxifen). The weighted vibrissae dominance index was unchanged in whisker-deprived DISC1cc animals receiving tamoxifen because the spared whisker responses did not potentiate (Figure 1, S2), and consequently the spared whisker domain did not expand into the deprived barrels surrounding the D1 barrel (Figure S3). The lack of plasticity in the DISC1cc mice was robust across two background strains

(Figure 1, S4). These results show that normal DISC1 interaction with Lis1 and Nudel is vital during a brief period in neonatal development for the adult animal to exhibit experience-dependent plasticity.

Transient disruption of DISC1/Lis1/Nudel interactions later in development had a smaller effect on L2/3 plasticity. Disrupting DISC1 C-terminal interactions at P11-13 reduced plasticity less than it did at P7 and had no effect at P28 (Figure 1D). This indicates that a critical period exists in early development with long lasting consequences for plasticity expressed much later in adulthood.

We studied the early development of the DISC1cc mice to see where the defect originated. We found that disrupting DISC1 C-terminal signaling at P7 retarded dendritic elongation and elaboration of dendritic branching (Figures S5, S6), but both had recovered by P21. The paired-pulse ratio, which is a measure of presynaptic maturation in the L4 to 2/3 pathway(17) was also delayed (Figure S7). Retardation of neuronal development demonstrates the immediate effect of disrupting DISC1 C-terminal interactions at P7, but does not explain the long lasting loss of adult plasticity.

The long-lasting effects of transient disruption of DISC1/Lis1/Nudel interactions were to be found at the level of the spines rather than the dendrites. At the start of the critical period for adult plasticity, the neurons highest order basal dendrites are mainly 2nd and 3rd order branches and are destined to become 50% of adult basal dendrites (Figure 2, S5, S6). We found lower spine density on 2nd and 3rd order dendritic spines in DISC1cc mice at P28 ($t_{(31)}$=2.36, p<0.03 and $t_{(41)}$=3.82, p<0.0005 respectively) and P50 ($t_{(30)}$=4.78, p<0.0001 and $t_{(43)}$=4.66, p<0.0001 respectively). The 4th and higher order dendrites, which mainly develop after the period during which we impaired DISC1 C-terminal interactions, showed normal spine density at P28 ($t_{(20)}$=0.96, p=0.35; interaction between dendrite order and genotype $F_{(4,104)}$=4.48, p<0.005) and at P50 ($t_{(30)}$=-1.318, p=0.20; interaction between dendrite order and genotype $F_{(4,117)}$=7.29, p<0.0001). The spine density deficit was only found on basal dendrites, not on apical dendrites ($F_{(4,131)}$=0.86, p=0.49).

The period when DISC1 C-terminal signaling is critical for adult plasticity (P7-P13) corresponds to a period of rapid synaptogenesis across the brain as well as in L2/3 of barrel cortex(18), when experience is necessary for AMPA insertion within synapses(19). Altered neonatal experience during this period leads to defocused receptive fields in adulthood(20). As the size of spine heads are correlated with their AMPA receptor content (21,22), we investigated spine head size and classification. There were fewer mushroom spines, (both as a percentage of the whole and in absolute terms) on the 2nd and 3rd order dendrites of DISC1cc mice than on their 1st, 4th and 5th order dendrites ($t_{(35.8)}$=8.76, p<0.0001), and fewer than on the 2nd and 3rd order dendrites of wild-type mice ($t_{(49.9)}$=8.72, p<0.0001). Furthermore, there were more thin spines on the 2nd and 3rd order dendrites in the DISC1cc mice ($t_{(75)}$=-3.07, p<0.005 compared to wild-types, and $t_{(68)}$=-4.10, p<0.0005 compared to other dendrite orders within the DISC1cc mice). Finally, the spine heads were smaller on the thin spines in the DISC1cc mouse 2nd and 3rd order dendrites than in the wild-types ($t_{(760)}$=3.31, p<0.01) (Figure 2). These findings imply a lower level of AMPA receptor insertion in DISC1 mutants.

We investigated synaptic function further in DISC1 mutants and found that while the AMPA/NMDA ratio followed a normal developmental trajectory up to P14, it diverged at P28 ($t_{(18)}$=2.33, $p<0.05$) and did not recover by P50 ($t_{(18)}$=3.29, $p<0.01$; Figure 3A). Consistent with this finding, silent synapses were present in DISC1 L2/3 cells at P50 (Figure 3B), whereas in wild-types they had converted to functional synapses by this age(23). The NMDA component of the synaptic response was also immature, containing a higher proportion of GluN2B versus GluN2A subunits than normal ($t_{(10)}$=3.9, $p<0.005$) (Figure 3C)(24). In contrast, inhibition appeared to be unaffected in DISC1cc mice (Figure S8). Low levels of GluN2A and AMPA receptors are consistent with the spine size defects and implies glutamate receptor insertion is affected by transient disruption of DISC1 C-terminal interactions in early development. These factors predict that synaptic plasticity should also be deficient in DISC1cc mice(21,22,25).

On investigation, we found that LTP was absent in the P7 tamoxifen-treated DISC1cc mice at P28 and P50 (Figure 3E.F) indicating that development of LTP was abolished rather than delayed. LTD was affected although not abolished: the time-course of LTD was slower and the probability of LTD induction was lower in DISC1cc mice (Figure S9), though it was possible to induce LTD in the mutants as in the wild-types (Figure 3G). This suggested that it might be possible to reverse LTD in these synapses despite their lack of LTP. Previous studies had shown that 7 days of complete bilateral whisker deprivation can occlude LTD in the barrel cortex and reset the synapses to a state that favors LTD reversal(26). We found it was possible to reverse LTD in the complete whisker deprived DISC1cc mouse (Figure 3H). These results show that developmental disruption of DISC1 signaling blocks or impairs selective aspects of synaptic plasticity.

Adult plasticity is different from many forms of developmental plasticity(27,28). In the somatosensory and visual cortex, adult plasticity is dependent on CaMKII and closely related to LTP(29,30). Developmental forms of synaptic plasticity such as TNFα dependent synaptic scaling, experience-dependent depression and LTD are gradually reduced with age(30,31). We found that the normal period of LTD expression in the barrel cortex ends between P50 and P100 (Figure 3D), after which LTD and reversal of LTD are not available modes of plasticity. Therefore, the loss of adult LTP only becomes critical at an age when developmental forms of plasticity have decreased to low levels. The latent effect of ablating prospective adult plasticity during an early critical period may therefore help explain the late onset of some schizophrenia symptoms.

How might a loss of LTP affect psychiatric conditions? Working memory is defective in schizophrenia and relies on persistent modes of network firing(32). Persistent neuronal activity requires formation of attractor states in neuronal networks, as has recently been shown in monkey pre-frontal cortex during context dependent integration of visual information(33). Therefore, a loss of plasticity such as we describe here is likely to disrupt working memory function by preventing formation of stable attractor states.

The C-terminal domain of DISC1 expressed in the DISC1cc mouse is known to reduce wild-type DISC1-Nudel and DISC1-Lis interactions(15). DISC1-Nudel interactions are thought to depend on the C-terminal domain's ability to form dimeric and tetrameric states(16). DISC1 and Nudel interact strongly at P7, less so by P16 and negligibly by 6 months(14). The DISC1-Nudel complex is therefore available to be disrupted only when spines form rapidly on cortical neurons during the critical period we describe here for adult plasticity. Nudel and DISC1 also both bind to Lis1 (14) and Lis1 haploinsufficiency has been shown to decrease spine density, specifically on 2^{nd} and 3^{rd} order dendrites(34) in striking similarity to the present results. Human iPS cells from schizophrenia and depression sufferers carrying a DISC1 C-terminal mutation also exhibit deficits in synapse formation(35). By restricting DISC1 C-terminal dysfunction to a short period of development, we have been able to show that adult plasticity (a) depends on synapse formation during this early critical period, (b) cannot be recovered despite continued expression of normal DISC1 and (c) is independent of DISC1-Nudel interactions in adulthood.

Figure legends.

Figure 1. Plasticity is impaired in adults by transient impairment of DISC1 C-terminal interactions at P7.

A) Whisker deprivation and expansion of spared whisker domain (orange area) (13) **B)** Weighted vibrissae dominance index (WVDI) for spared versus principal whiskers across experimental groups (total n=52 mice, 496 cells. Naïve mice = black bars, deprived mice = gray bars). WVDI increases with deprivation except for in DISC1cc mice injected with tamoxifen at P7 [$F_{(7,51)}$=10.6, p<0.001, 3-way ANOVA]. Tamoxifen only affected plasticity in DISC1cc mice and not wild-types (interaction between genotype and tamoxifen (p<0.0005)). **C)** WVDI increased with deprivation (gray bars) directly correlated with spared (D1) whisker potentiation (R=0.93, p<0.0001). **D)** The WVDI increases in DISC1cc mice injected with Tamoxifen on P11-13 ($t_{(12)}$=4.97, p<0.05, black = naïve, gray = deprived) but only attains levels seen in WTs (red square) when injected at P28 (P7 injected WTs not different from P28 injected DISC1s, $t_{(12)}$=0.61, p=0.45) [interaction between age and deprivation $F_{(2,2)}$=10.46, p<0.0003, ANOVA]. The WT control data is plotted at P45 for clarity (red = deprived, blue = naïve) but all mice were injected with tamoxifen at P7. All plasticity values were measured in adulthood.

Figure 2. Enduring effects of transient impairment of DISC1 C-terminal interactions at P7 on dendritic spines.

A) Example of L2/3 dendrites showing spines and dendritic order. Scale bar = 10um **B)** DISC1cc mice had lower spine density on second and third order dendrites at P28 and P50. Spine density was lower at P8 on third order dendrites in DISC1cc mice. (* p<0.05, ** p<0.01, *** p<0.001). **C,D)** DISC1cc mice had a lower density of mushroom spines and a higher density of thin spines on 2nd and 3rd order dendrites. (ANOVA: interaction between dendrite order and genotype for mushroom spines: $F_{(1,124)}$=58.64, p<0.0001 and for thin spines $F_{(1,124)}$=7.40, p<0.01).

Figure 3. Persistent functional consequences of transient impairment of DISC1 C-terminal interactions at P7.

A) The AMPA/NMDA ratio of WT and DISC1cc mice diverge after P14 and this ratio in DISC1cc mice remains at a low level into adulthood (P50 WT ratio 8.29 ± 0.97, DISC1 ratio 4.52 ± 0.61, $t_{(15)}$=3.29, p<0.01). **B)** 50% of P50 DISC1 recordings had minimal-stimulus EPSC success rates at +40mV higher than at -70mV, indicative of the presence of silent synapses. **C)** NMDA currents in adult DISC1cc mice (red bar) showed enhanced sensitivity to ifenprodil application when compared to WT mice (black bar; DISC1 0.67 ± 0.08, WTs 1.01 ± 0.04, $t_{(10)}$=3.9, p<0.005). **D)** LTD in WT

mice was consistent between P14, P28 and P50 but was absent at P100 (average depression of 47 ± 13% at P14 ($p<0.01$), 47 ± 6% at P28 ($p<0.001$), 36 ± 6% at P50 ($p<0.001$) and -1 ± 14% at P100 ($p>0.05$)). **E)** Normalised peak EPSP amplitude is plotted versus time. Transient expression of mutant DISC1 at P7 abolishes the capability for inter-columnar LTP in layer 2/3 at P28 and **F)** at P50 (effect of genotype $F_{(1,74)}=14.27$, $p<0.0003$, not age $F_{(1,74)}=0.13$, $p<0.71$, ANOVA). The percentage of cells showing statistically significant LTP drops from 33% in wild-type mice to 5% in DISC1cc mice (P28) and 43% in wild-type mice to 9% in DISC mice at P50 (see pie charts). **G)** Average LTD values are similar in WT and DISC1cc mice ($F_{(1,18)}=3.44$, $p<0.08$, ANOVA), though the percentage of cells showing LTD drops from 90% in wild-types to 40% in DISC1. **H)** Complete whisker deprivation unmasks PKA dependent LTD reversal (26) and this is unaffected in the adult mouse by P7 DISC1cc ($F_{(1,19)}=0.16$, $p<0.87$, ANOVA).

References

1 Millar, J. K. et al. Human molecular genetics 9, 1415-1423, (2000).

2 Bradshaw, N. J. & Porteous, D. J. Neuropharmacology 62, 1230-1241, (2012).

3 Miyoshi, K. et al. Biochemical and biophysical research communications 317, 1195-1199, (2004).

4 Taya, S. et al. J Neurosci 27, 15-26, (2007).

5 Burdick, K. E. et al. Human molecular genetics 17, 2462-2473, (2008).

6 Hayashi-Takagi, A. et al. Nat Neurosci 13, 327-332, (2010).

7 Kang, E. et al. Neuron 72, 559-571, (2011).

8 Lipina, T. V. et al. Neuropharmacology 62, 1252-1262, (2012).

9 Schurov, I. L. et al. Molecular psychiatry 9, 1100-1110, (2004).

10 Kirkpatrick, B. et al. J Comp Neurol 497, 436-450, (2006).

11 Carlisle, H. J. et al. J Neurosci 31, 16194-16207, (2011).

12 Wang, Q. et al. Molecular psychiatry 16, 1006-1023, (2011).

13 Glazewski, S. et al. Science 272, 421-423, (1996).

14 Brandon, N. J. et al. Molecular and cellular neurosciences 25, 42-55, (2004).

15 Li, W. et al. Proc Natl Acad Sci U S A 104, 18280-18285, (2007).

16 Soares, D. C. et al. The Journal of biological chemistry 287, 32381-32393, (2012).

17 Cheetham, C. E. & Fox, K. J Neurosci 30, 12566-12571, (2010).

18 Micheva, K. D. & Beaulieu, C. J Comp Neurol 373, 340-354, (1996).

19 Wen, J. A. & Barth, A. L. J Neurosci 31, 4456-4465, (2011).

20 Stern, E. A. et al. Neuron 31, 305-315, (2001).

21 Nusser, Z. et al. Neuron 21, 545-559, (1998).

22 Kopec, C. D. et al. J Neurosci 27, 13706-13718, (2007).

23 Hardingham, N. & Fox, K. J Neurosci 26, 7395-7404, (2006).

24 Carmignoto, G. & Vicini, S. Science 258, 1007-1011, (1992).

25 Bellone, C. & Nicoll, R. A. Neuron 55, 779-785, (2007).

26 Hardingham, N. et al. Neuron 60, 861-874, (2008).

27 Fox, K. Neuroscience 111, 799-814, (2002).

28 Sato, M. & Stryker, M. P. J Neurosci 28, 10278-10286, (2008).

29 Hardingham, N. et al. J Neurosci 23, 4428-4436, (2003).

30 Ranson, A. et al. Proc Natl Acad Sci U S A 109, 1311-1316, (2012).

31 Otsuki, J. et al. Chemical communications, 608-609, (2003).

32 Durstewitz, D. et al. Nat Neurosci 3 Suppl, 1184-1191, (2000).

33 Mante, V. et al. Nature 503, 78-84, (2013).

34 Sudarov, A. et al. EMBO molecular medicine 5, 591-607, (2013).

35 Wen, Z. et al. Nature, (2014).

Supplementary Materials

www.sciencemag.org

Materials and Methods

Figs. S1-S9

References (36-46)

Acknowledgements

We should like to acknowledge the support of the MRC and NIMH to KF for this work. We should like to thank Tim Gould for histology, Alcino Siva for discussions on DISC1cc and Simon Butt for suggestions on methods of tamoxifen delivery. Supplement contains additional data.

Figure 1

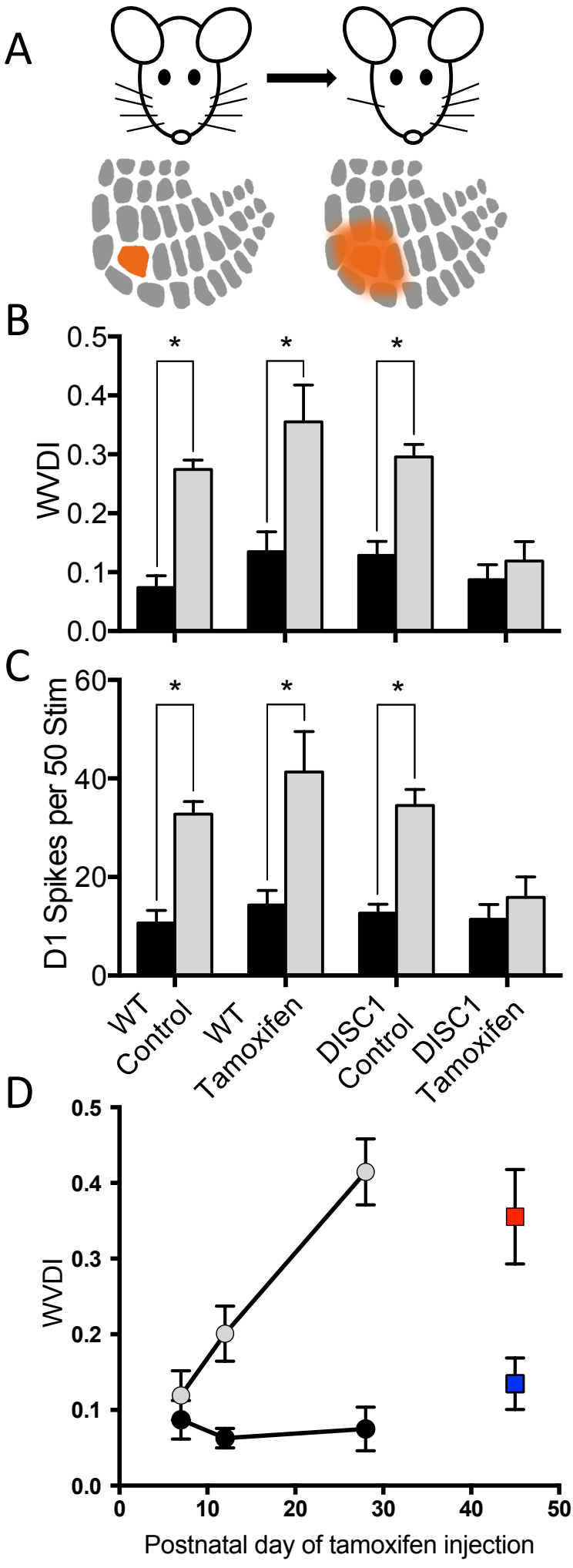
A
B
WVDI
0.5
0.4
0.3
0.2
0.1
0.0
*
*
*
C
D1 Spikes per 50 Stim
60
40
20
0
*
*
*
WT Control
WT Tamoxifen
DISC1 Control
DISC1 Tamoxifen
D
WVDI
0.5
0.4
0.3
0.2
0.1
0.0
0
10
20
30
40
50
Postnatal day of tamoxifen injection

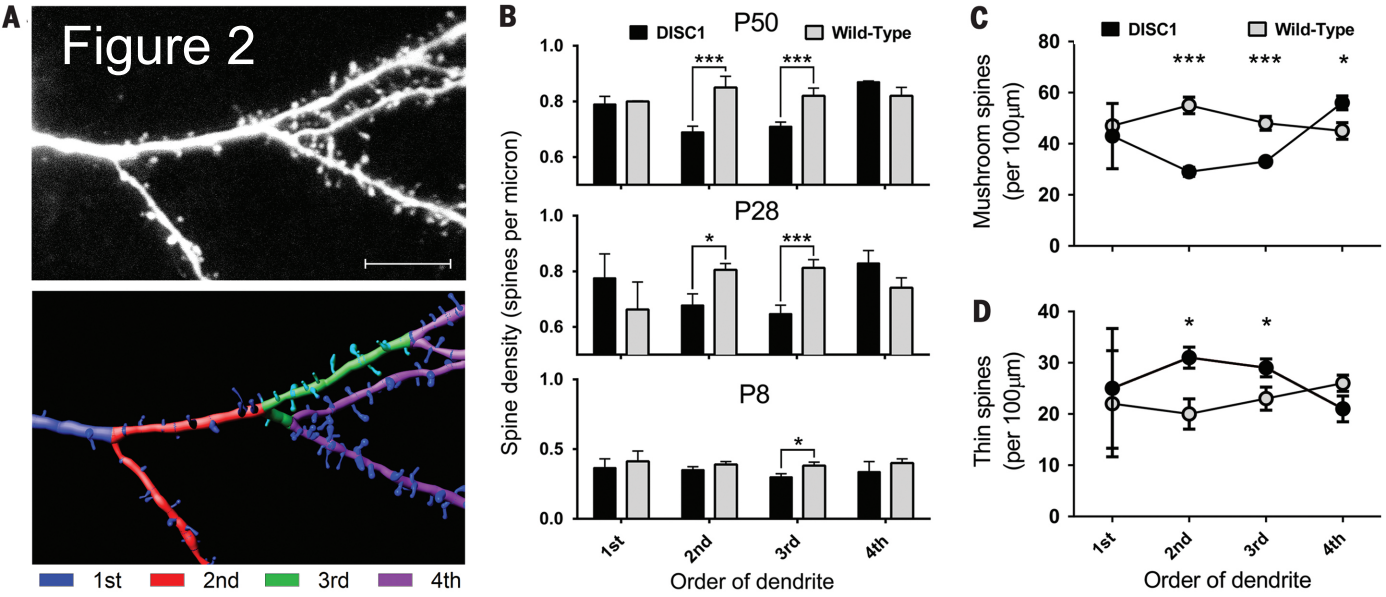
A
Figure 2
1st
2nd
3rd
4th
B
DISC1
Wild-Type
P50
P28
P8
Spine density (spines per micron)
Order of dendrite
C
Mushroom spines (per 100μm)
D
Thin spines (per 100μm)

Figure 3

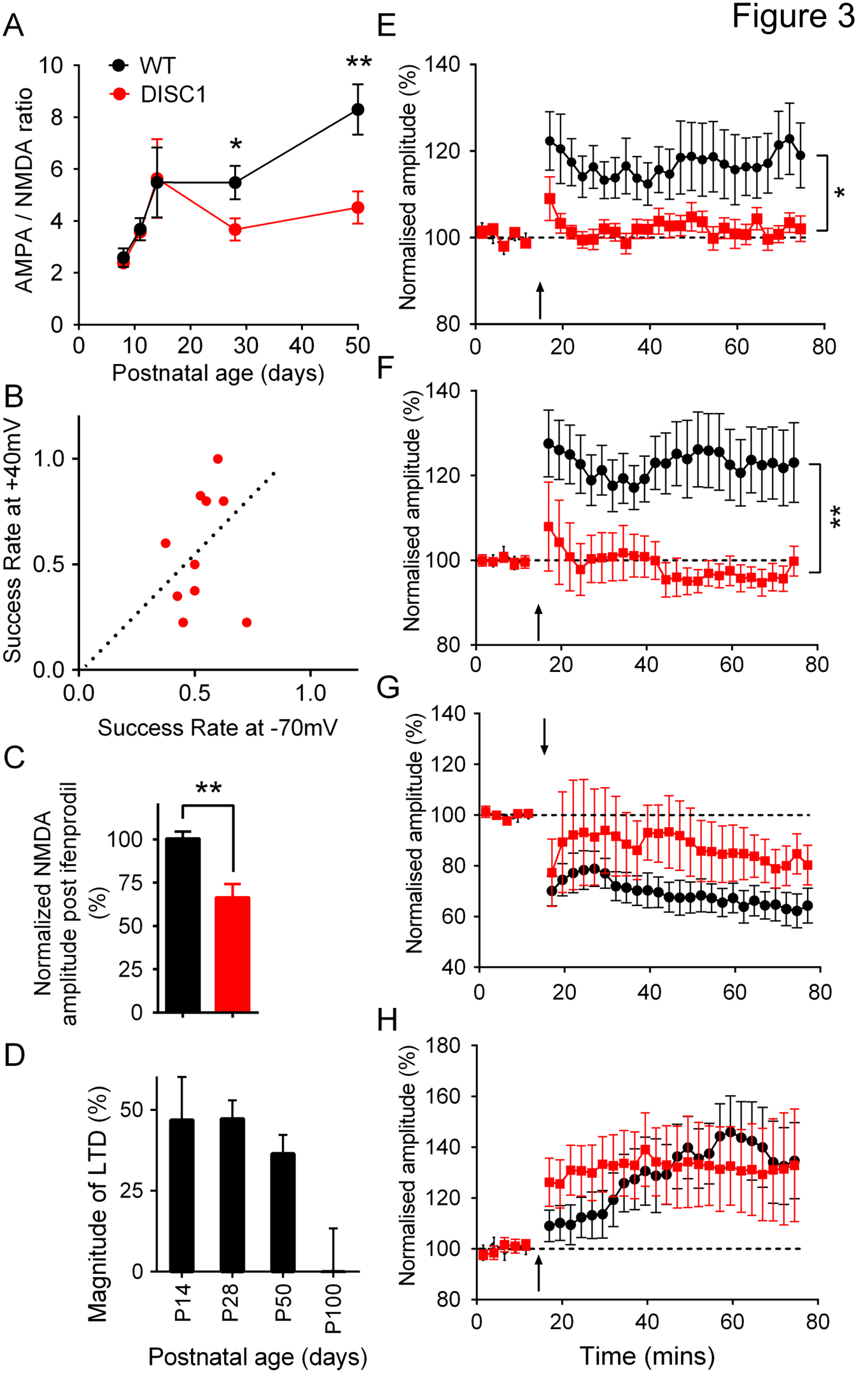
A
WT
DISC1
AMPA / NMDA ratio
Postnatal age (days)
B
Success Rate at +40mV
Success Rate at -70mV
C
Normalized NMDA amplitude post ifenprodil (%)
D
Magnitude of LTD (%)
P14
P28
P50
P100
Postnatal age (days)
E
Normalised amplitude (%)
F
Normalised amplitude (%)
G
Normalised amplitude (%)
H
Normalised amplitude (%)
Time (mins)

Materials and Methods

Subjects

Tamoxifen-inducible DISC1cc mice (15) were obtained from Alcino Silva at UCLA and maintained by inbreeding or crossbreeding with C57Bl/6J mice (Harlan Labs, UK) or C57Bl/6N mice (Taconic, Ry, Denmark). Animals were social-group housed with *ad libitum* food and water in a 12:12 hour normal light/dark cycle. Both male and female mice were used throughout the study. All animal care and use was performed in compliance with the UK Animals (Scientific Procedures) Act 1986.

Transgene induction

Mice received a single subcutaneous (s.c.) injection of tamoxifen (20 mg/kg, Sigma, UK) in corn oil at postnatal day 7, or 28 or for the P11-13 group, one injection on P11 and one on P13. Control animals received s.c. injections of corn oil on the same postnatal days. Both transgenic animals and their wild-type littermates were used to control for any possible effects of tamoxifen on plasticity and neurophysiology.

Whisker Deprivation

Mice (aged P50-75 at start of deprivation) were briefly anaesthetised with isoflurane for 1-2 minutes. The vibrissal pad was visualised under a dissecting microscope and the whiskers removed by a gentle pulling motion to leave the follicle intact. This process does not damage the follicle innervation and allows the whisker to regrow(36). The process was repeated every 2-3 days as necessary to remove any regrown whiskers. For *in vivo* plasticity studies the whiskers on the right-hand side were deprived with only the D1 whisker spared to provide a period of single whisker experience for 18 days (with 5-7 days regrowth after). For *in vitro* studies all whiskers were removed bilaterally for 7 days.

In vivo electrophysiology

Subjects: Anaesthesia was induced with isoflurane and maintained by urethane (1.5g/kg body weight i.p. with a trace amount of acepromazine) in adult mice (age range P50-113, n=89). Hindlimb and corneal reflexes, breathing rate and cortical activity were used to monitor anaesthesia levels and maintain animals in a state similar to stage 3-4 sleep(37). Supplemental doses of urethane (10% initial dose)

were administered as required. Topical analgesic (lidocaine) was applied to the ears and scalp.

Surgery: Anaesthetised mice were placed in a stereotaxic frame (Narashige, Japan) and body temperature maintained at 37ºC throughout surgery and recording by a thermostatically controlled heating blanket (Harvard Apparatus, Kent, UK). A 2x2mm section of the left parietal cranium was thinned with an electric dental drill over the barrel cortex (0-2mm caudal from bregma, 2-4mm lateral from midline). A small fleck of thinned skull was removed from the area with a 30G hypodermic needle to create a hole just large enough to allow the carbon fibre electrode access for each penetration. The dura was left intact as the electrode was strong enough to break through it without resection.

Recordings: Carbon-fibre electrodes(38) were used to make recordings from barrels corresponding to those whiskers immediately surrounding the spared whisker. Recordings were made at even intervals of 50μm from the surface to the bottom of layer 4. Action potentials were amplified with a Neurolog system isolated using a window discriminator to provide single-unit recordings (Digitimer, Welwyn Garden City, UK) and digitised with a CED 1401 and Spike2 software (CED, Cambridge, UK) running on a Windows desktop PC. Whiskers were stimulated one at a time using a glass rod attached to a piezo wafer driven by a Digitimer DS-2 isolated stimulator. Stimuli were applied as single 10ms 200μm upward deflections at 1Hz, repeated 50 times.

Histology: The locations of the extracellular recording penetrations were confirmed by micro-lesions made at the end of each recording penetration. Small electrical lesions (1 μA DC, tip negative, 10 seconds) were made at an estimated depth of 350μm. At the end of the recording session the mouse was deeply anaesthetised and transcardially perfused with 0.1M phosphate-buffered saline, followed by 4% formaldehyde in PBS. The brain was removed after fixation and the recorded hemisphere's cortex dissected and flattened between two glass slides as previously described (39). The flattened cortex was then postfixed for 24h in 4% formaldehyde/20% sucrose in PBS and then transferred to 20% sucrose PBS until sectioning. Tangential sections (35μm) were cut on a freezing microtome and stained for cytochrome oxidase activity by reaction with diaminobenzidine and cytochrome C

(40). The lesions from recording were then correlated with the histology to confirm in which barrel each cell was recorded.

***In vitro* methods**

A total of 287 mice aged between 8 and 70 days old were used (WT and DISC1cc mice both injected with tamoxifen at P7). Recordings were analysed from 960 cells. For experiments carried out following whisker deprivation, we used a deprivation period of 7 days as this has been shown to have the greatest effect on layer 2/3 cortical plasticity (41) (see above for deprivation methods).

In vitro recording conditions and stimulation protocols

Coronal slices (400µm thick) containing barrel cortex were taken from mice using a Micron MM650V microtome (Thermo-Scientific, UK). Slices were maintained in a submersion chamber continually perfused (2-3ml/min) with artificial cerebro-spinal fluid (ACSF) containing (in mM): 119NaCl, 3.5KCl, 1NaH_2PO_4, 2$CaCl_2$, 1$MgSO_4$, 26$NaHCO_3$, 10 glucose and 10μM picrotoxin to block IPSPs. The solution was bubbled with 5% CO_2-95% O_2 and slices were kept at room temperature (21-24ºC). Intracellular electrodes contained (in mM): 110 K-gluconate, 10KCl, 2$MgCl_2$, 0.3 Na_2ATP and 0.03 NaGTP. Biocytin (Sigma, UK) was routinely added to the electrode filling solution at a concentration of 5mg / ml. Electrode resistance was 10-15MΩ.

Slices were placed in the recording chamber under an upright microscope (BX 50 WI, Olympus, UK). Pyramidal neurons were chosen in layer 2/3 of the somatosensory cortex directly above the layer IV barrels under visual guidance, using a 40x water immersion objective, differential interference contrast (DIC) optics and infrared illumination. Whole-cell recordings were made from pyramidal cells in the current clamp configuration. Signals were amplified using an Axoclamp 2B amplifier (Axon Instruments, USA), low pass filtered at below 1-3kHz (Digitimer, UK) and sampled at 5kHz for analysis off-line on a PC computer (RM, UK).

After recordings were obtained, the neurons were electrophysiologically characterised. Firstly, the input resistance of the neuron was recorded by injection of long pulses of current. I/V relationships of cells were obtained by injecting varying negative and positive sub-threshold currents into the neurons. Postsynaptic action potentials were measured in response to long pulses of depolarising current injection.

Responses to short hyperpolarising pulses of current were also measured in order to calculate the final time constant of the membrane. The series resistance was continually monitored during the recording and recordings were rejected if it changed by over 20% during the experiment.

The identity of neurons as pyramidal was subsequently confirmed by histological processing. After neurons had been electrophysiologically identified as pyramidal, monosynaptic EPSPs were evoked via a monopolar stimulating electrode placed accurately in layer 4 of either the home barrel or the adjacent barrel column. The stimulus intensity was adjusted to produce an EPSP amplitude of roughly 5mV in the postsynaptic neuron. Monosynaptic components of EPSPs were recorded and had reversal potentials close to 0 mV (-2 ± 3 mV). Trains of EPSPs were evoked in responses to 10 stimuli at 10Hz or 20 stimuli at 20Hz and amplitudes measured post-hoc in order to quantify short-term plasticity.

Plasticity Experiments

For LTP experiments, after a control period of recording (stimulating at a frequency of 0.1Hz), the post-synaptic neuron was subjected to a paired pre- and post-synaptic spiking protocol, where the presynaptic stimulus was timed to occur 10ms before a postsynaptic action potential evoked by somatic current injection. This pre-post interval has been shown to be effective in inducing LTP in layer 2/3 barrel cortex of a similar age to the current study (41) Trains of paired activity consisted of 50 paired action potentials at a frequency of 2Hz. The paired pulse ratio was defined as being the peak amplitude of the second EPSP divided by the peak amplitude of the first EPSP. The LTP protocol consisted of four sets of trains of paired activity with a minute between the trains. After the pairing protocol, the evoked EPSP was again recorded for a further hour. For LTD experiments, the post-synaptic action potential was timed to occur 50ms before the presynaptic stimulation. As LTD is difficult to induce in mature brain slices, the protocol consisted of 800 reverse-paired stimulations at 2Hz. When investigating the age dependence of LTD, the same LTD experiment was performed on P14, P28, P50 and P100 cortex.

EPSP Measurement

EPSPs were measured using an automated routine that compared a window in the baseline membrane potential shortly before the EPSP with the peak EPSP amplitude. Amplitudes were binned into 30 second epochs for data analysis.

AMPA to NMDA ratios

AMPA to NMDA ratios of evoked EPSPs were obtained pharmacologically (42). At resting membrane potentials, EPSPs were mediated by AMPA currents and entirely blocked by addition of CNQX to the ACSF. Stable periods of AMPA mediated potentials were recorded under control conditions and then AMPA mediated EPSPs were blocked and NMDA mediated EPSPs simultaneously unmasked using a modified ACSF solution containing 0mM magnesium and 20μM CNQX or 10μM NBQX. Rise times and half widths of PSPs were recorded and confirmed the existence of AMPA and NMDA potentials. Potentials recorded in zero magnesium and CNQX were entirely blocked by 50 μM APV. Ratios were calculated of the amplitudes of the AMPA mediated and NMDA mediated potentials (42). In order to calculate the NR2B component of the NMDA mediated PSPs, PSPs were recorded before and after application of 3μM ifenprodil (43) and stable periods of recording in control conditions and after perfusion of ifenprodil were averaged and the reduction in NMDA EPSPs calculated.

IPSC recordings

During recordings of layer 2/3 neurons, slices were perfused with oxygenated ACSF containing 2mM kynurenic acid and 1μM tetrodotoxin to block ionotropic glutamate receptors and voltage-gated sodium channels, respectively. We recorded a population of spontaneously occurring inward currents at the normal resting potentials (-70mV) using a high chloride containing intracellular solution (140mM CsCl, 4mM NaCl, 10mM HEPES, 1mM $MgCl_2$,2mM Ma-ATP, 0.05mM EGTA) from 4 week old mice (44). Currents were completely blocked by the $GABA_A$ receptor antagonist picrotoxin (50μM). mIPSCs amplitudes and frequencies were measured for 100 second epochs of recording and averaged between genotypes and animal. The threshold for event detection was set at two to three times the signal to noise ratio at 5pA.

Silent Synapses

Recordings measuring the incidence of silent synapses were made as previously described (23). Layer II/III pyramidal cells (n = 10) from tamoxifen-treated (P7) DISC1-cc animals were patched in voltage clamp mode, with the addition of 5mM QX-314 in the intracellular solution. A unipolar stimulating electrode was placed in layer IV directly below the patched cell and EPSCs evoked at 0.1 Hz. Stimulus intensity was reduced until a failure rate of approximately 50% was observed at a holding potential of -70 mV. Forty EPSCs were then evoked at -70 mV holding and the success rate noted. Holding potential was changed to +40 mV and the cell allowed to equilibrate for 2-3 minutes (until holding current stabilised). Forty more EPSCs were evoked with the same stimulus parameters and the success rate at +40 mV noted. EPSC success rates were then compared for the two holding potentials; if there was a higher probability of evoking an EPSC at depolarised potential then the cell was considered to contain silent synapses.

Anatomical reconstructions

Following recordings, slices were fixed overnight at 4ºC in 100 mM phosphate buffered saline (PBS, pH 7.3) containing 4% paraformaldehyde (BDH, USA). Slices were then transferred to PBS and histologically reconstructed by conventional methods described previously (41). Slices were incubated for 30 minutes in PBS with 0.3% hydrogen peroxide containing 0.4% Triton X-100 (Sigma, UK). They were then washed in PBS with Triton and then incubated for 2 hours in PBS-avidin-biotinylated horseradish peroxidise (ABC, Vector Labs, USA). Slices were then reacted using 3,3-diaminobenzidine (DAB, Sigma, UK) using nickel as the chromogen until the soma and dendritic arborisations were clearly visible (viewed under the light microscope, Olympus, UK). After several further rinses in PBS the sections containing the neurons were mounted on slides.

Morphological reconstructions of biocytin-filled neurons

The 2D representation of the cells was achieved using a camera lucida (Olympus, UK) drawing of the filled neurons (Figs. 2a & 2b). The neurons' dendritic fields were then analysed using Sholl analysis(45). We measured the number of occasions that dendrites crossed the Sholl shells at increasing distances from the soma (dendritic counts(41)).

Measurements of spine density and classification

Neurons were filled with biocytin and fixed with paramformaldehyde in an identical manner to that used for dendritic quantifications. Thereafter, slices were incubated for 18 hours in PBS supplemented with 1% Triton X-100 and 0.2% streptavidin Alexa Fluor 488 conjugate (Invitrogen) at 4-6ºC (46). After washing with PBS, cells were located in slices under a fluorescent microscope and subsequently imaged under a 2-photon microscope (Prairie Systems) and spine density measured from z stacks (ImageJ). Spines were classified into four groups (mushroom, thin, and stubby spines, and filopodia) based on head-to-neck ratio and neck length (Mushroom spines – head:neck ratio >1.15, neck length <0.09μm; thin spines - head:neck ratio >1.15, neck length >0.09μm, stubby spines: head:neck ratio <1.15 and length <1.1μm). Filopodia were easily distinguished by having no detectable spine head, were infrequent and not included in this report. Further spine analysis was conducted using Imaris software (Bitplane, Andor Technology, Belfast).

Layer depth and cell density measurement

WT and DISC1cc mice previously subjected to tamoxifen injection at P7 were transcardially perfused at P50-P70 (n=4 per group) and fixed as described above. Coronal sections were cut at 40μm on a freezing microtome and transferred to PBS. Sections were mounted on subbed slides, defatted with acetone and processed for Nissl staining (Thionin, 1%).

NeuN immunostaining for cell density: Sections were blocked in 5% Normal Goat Serum in 0.1M PBS and 0.1% TritonX-100 for 1 hour. After blocking sections were incubated in a primary antibody mix (in 0.1M PBS, 0.1% TritonX-100 and 3% Normal Goat Serum) of mouse monoclonal anti-NeuN (Millipore MAB377, 1:100 dilution) for 2 hours at room temperature, 18 hours overnight at 4ºC and a further 2 hours at room temperature. After 3x 30 minute washes in 0.1M PBS and 0.1% TritonX-100 the secondary antibody Alexa594 goat anti-mouse (Life Technologies A11032, 1:200 dilution) was applied (in 0.1M PBS , 0.1% TritonX-100 and 3% Normal Goat Serum). Slices were incubated in the secondary mix for 3.5 hours at room temperature, and then after a further 3x 20 minute washes in 0.1M PBS and 0.1% TritonX-100 were mounted in Vectashield DAPI hardset (Vector H1500). The same protocol was applied to tangential slices alternating with slices stained for cytochrome oxidase to localise viral spread across barrels.

Sections were visualized using a Leica TCS SP2 confocal microscope. Cell density in confocal images was automatically quantified with Imaris F1 7.7.2 (Bitplane, Andor Technology, Belfast).

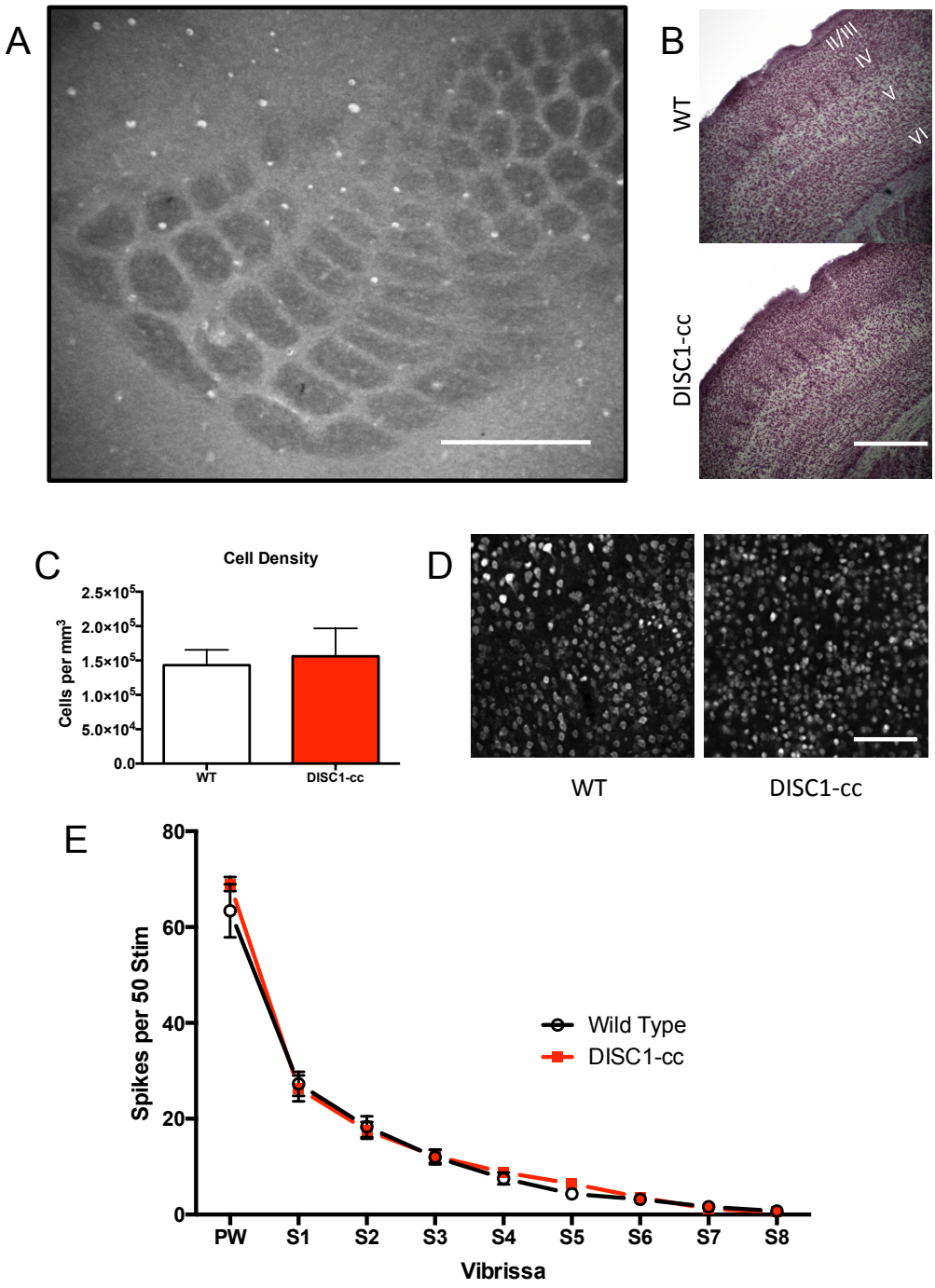

Figure S1. Development of the barrel cortex is normal at the macroscopic scale in animals with transient expression of mutant DISC1 at P7.

A) The normal barrel cortex pattern develops in Layer 4 in DISC1cc mice as shown with this cytochrome oxidase stained section. The area of the D1-D5 barrels were measured in wild-types and DISC1cc mice that had either been treated with

tamoxifen or vehicle; values were compared across tamoxifen treatment and genotype and were found not to be different (no effect of tamoxifen $F_{(1,18)}$=0.05, p=0.81; no effect of genotype $F_{(1,18)}$=0.63, p=0.44, 2-way ANOVA). Note the micro-lesion made in the C1 barrel to mark the location of the recording penetration (scale bar = 500μm). **B)** Cortical layers have the same thickness in DISC1cc mice as in WTs as shown in these Nissl stained coronal sections of barrel cortex. The depth of the junctions between layers was measured for DISC1cc and WT mice and found to be similar in absolute thickness (microns) and in thickness relative to the total cortical depth (L2/3 thickness: WT 313$\pm$11μm, DISC1cc 334$\pm$6 μm; L2/3/4 thickness: WT 458$\pm$6μm, DISC1cc 453$\pm$8μm; total cortical depth: WT 987μm, DISC1 979μm) (L2/3, $F_{(1,6)}$=1.7, p=0.22; L2/3/4, $F_{(1,6)}$=0.005, p=0.94) (scale bar = 500μm). NB: this is in contrast to studies where DISC1 mutations are active during cell migration, which results in thinner L2/3 (1) **C)** Layer 2/3 cell densities are similar between DISC1cc mice as in WTs ($F_{(1,14)}$=0.62, p=0.44). **D)** Examples of barrel cortex in DISC1cc and WT mice showing the similarity of cell density between genotypes (neurons labelled with Neu-N; scale bar = 100μm). **E)** Receptive field profiles for undeprived WT and DISC1cc mice. The responses are plotted in order from the anatomically defined principal whisker (PW) and then by the greatest to least responding surround whisker (S1, S2, … S8). There were no differences in adulthood between the undeprived receptive fields in WTs and DISC1cc mice treated with tamoxifen at P7.

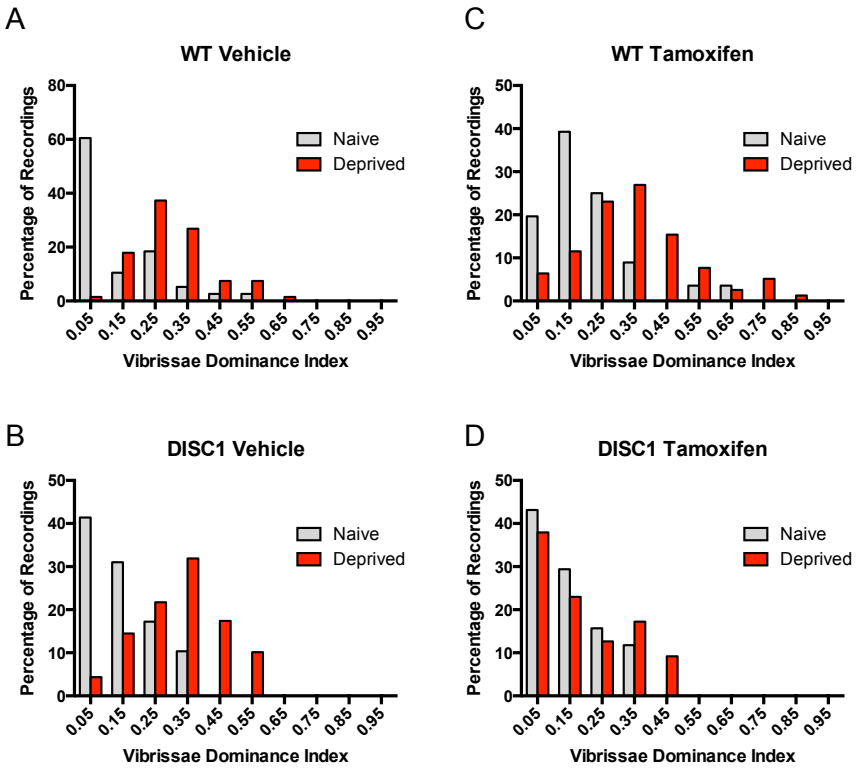

Figure S2. Vibrissae dominance histograms show P7 activation of DISC1cc impairs adult plasticity.

A, B) Vibrissae dominance histograms for adult WT and DISC1cc mice treated with corn oil vehicle at P7. Naïve mice display a left-shifted dominance histogram as the average PW response far outweighs the D1 response (see Figure 1). Modal VDI was 0.05 for both WT and DISC1cc naïve vehicle-treated mice. After 18 days D1-spared deprivation the modal VDI was 0.25 for WT and 0.35 for DISC1cc vehicle-treated mice. **C)** WT mice treated with tamoxifen at P7 still displayed a large shift in VDI after 18 days single whisker experience (modal VDI = 0.15 naïve, 0.35 deprived) **D)** In contrast to the other cohorts, DISC1cc mice treated with tamoxifen at P7 did not exhibit a VDI shift in deprived animals (modal VDI = 0.05 for both naïve and deprived groups) suggesting that adult experience-dependent plasticity is abolished in these animals.

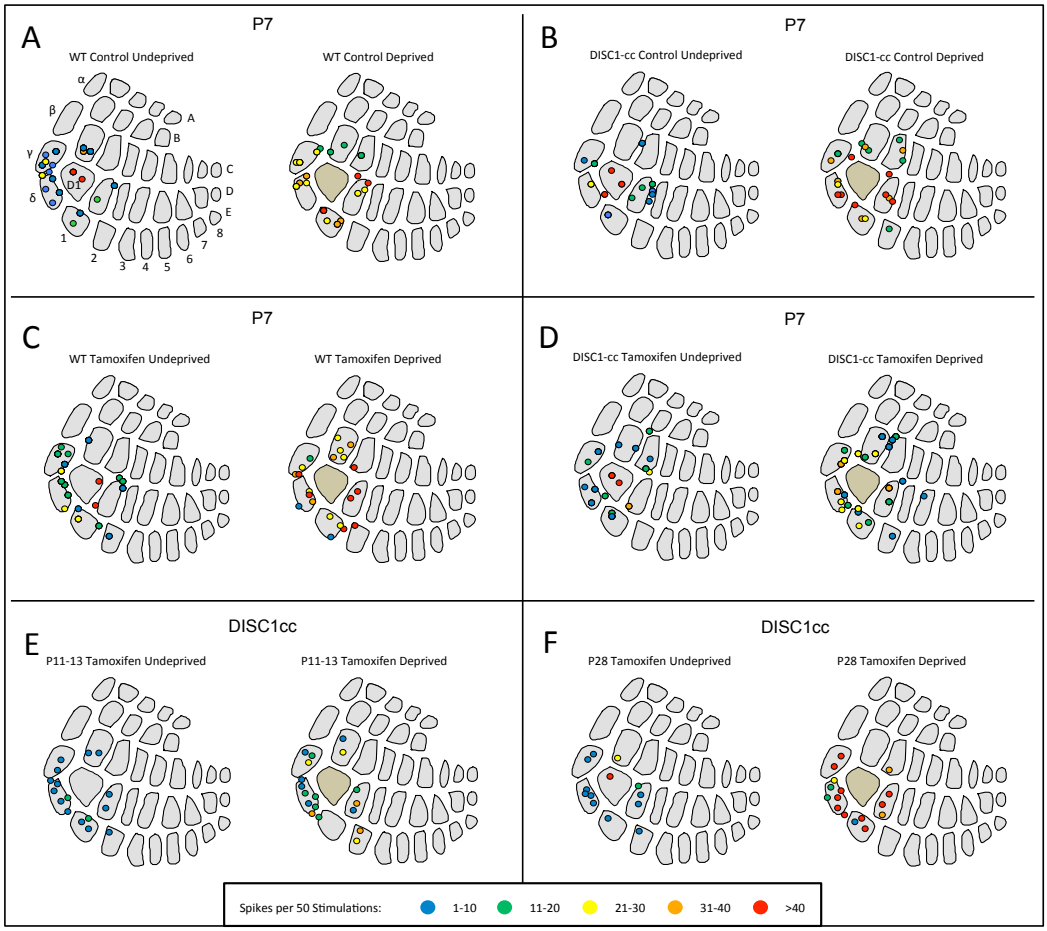

Figure S3. Penetration maps showing the average spike rate of recorded cells to D1 whisker stimulation.

The heat map indicates the strength of responses within a penetration (key below figure). Deprived animals exhibiting experience-dependent plasticity would be expected to show a greater spike rate in response to spared whisker stimulation in the barrels surrounding D1. **A)** In vehicle treated wild-type mice, the proportion of penetrations with a mean spike rate of 31 or above (per 50 stimulations) is 1/18 in naïve mice and 6/19 in deprived animals (5.5% vs 31.6%, $\chi^2(1,37) = 4.08$, $p < 0.05$, Pearson's chi-square test). **B)** Similarly, in vehicle treated DISC1cc mice, 1/12 penetrations were high-spiking in control mice and 13/21 responded strongly to D1 stimulation in deprived animals (8.3% vs 61.9%, $\chi2(1,34) = 9.74$, $P < 0.01$, Pearson's chi-square test). **C)** Treatment of WT mice with tamoxifen at P7 did not ameliorate the shift in favour of D1 in deprived animals, with 1/18 cells responding strongly to D1 stimulation in naïve mice and 11/21 in deprived mice (5.5% vs 52.4%, $\chi2(1,39) = 9.98$, $P < 0.01$, Pearson's chi-square test). **D)** In contrast to the control conditions shown in A-C, treatment of DISC1cc animals with tamoxifen at P7 resulted in no

difference in the proportion of strong D1-responding penetrations when comparing naïve and deprived mice, suggesting a deficit in experience dependent plasticity (Naïve = 1/15, 6.6% vs deprived 2/22, 9.1%, $\chi2(1,37) = 0.07$, $P > 0.05$, Pearson's chi-square test). **E)** DISC1-cc mice treated with tamoxifen at P11-13 did not show a significant difference in the proportion of highly responsive cells between naïve and deprived animals (Naïve = 0/16, 0% vs deprived 3/18, 16.7%, $\chi2(1,34) = 2.92$, $P = 0.087$, Pearson's chi-square test), although other measurements of plasticity (e.g. weighted vibrissae dominance) suggest that some experience-dependent plasticity does occurs in this group (Figure 2, main text). **F)** Treatment with tamoxifen at P28 did not hinder experience-dependent plasticity, with deprived mice showing a significantly higher proportion of D1-biased penetrations (Naïve = 0/12, 0% vs deprived 12/16, 75%, $\chi2(1,28) = 15.75$, $P > 0.0001$, Pearson's chi-square test).

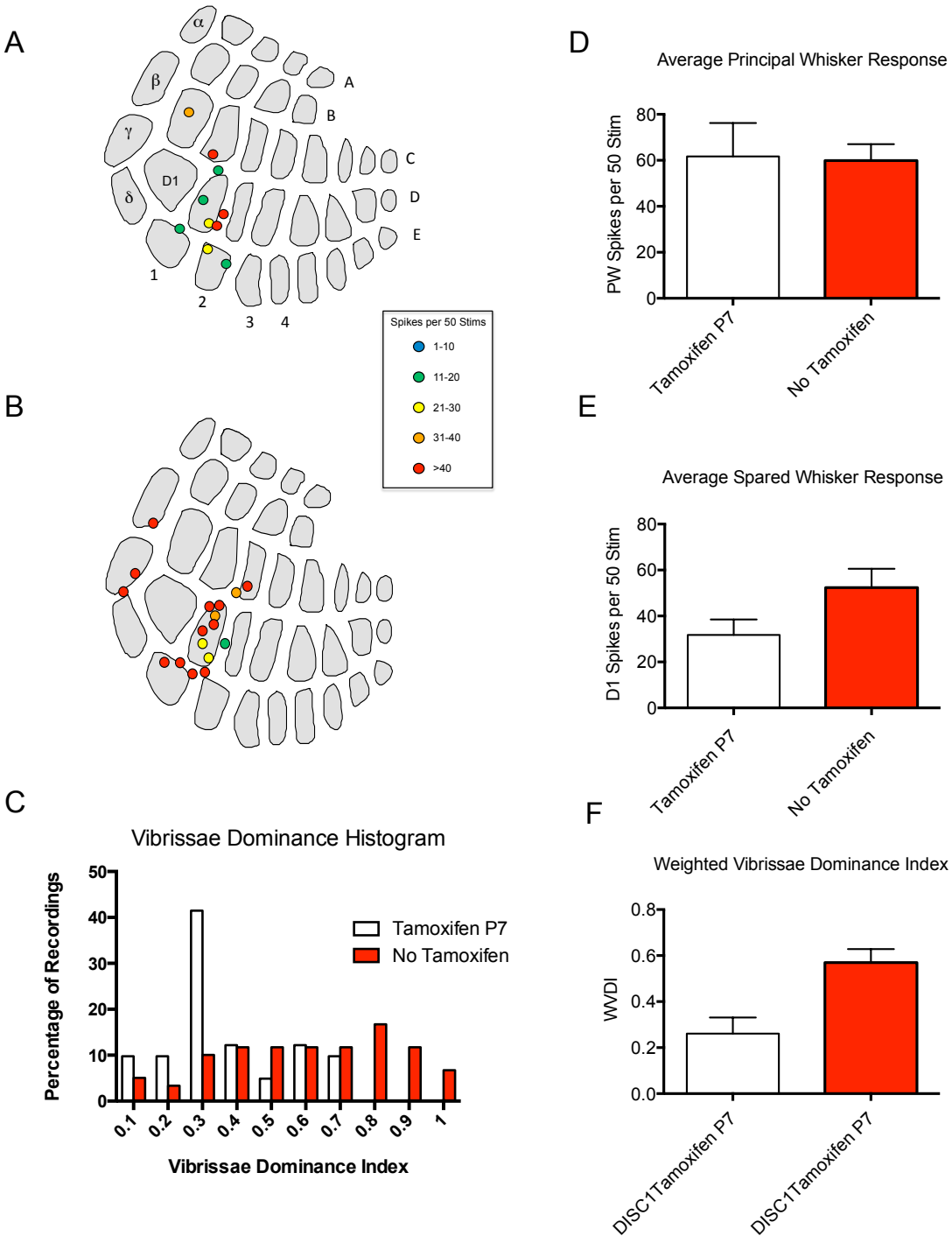

Figure S4. Transient DISC1cc expression at P7 blocks experience-dependent plasticity in mice with a different background strain from those shown in Figure 1.

DISC1cc mice were bred to a C57BL/6N Taconic background. Mice were either injected with tamoxifen **(A**) or vehicle control on P7 **(B)**. **A)** The aggregate penetration map is show for recordings from 6 animals. The colour code shows the average response of L2/3 cells in a particular penetration (cells recorded at 50 micron intervals from 50 microns to 250 microns depth in each penetration). Many

fewer penetrations show potentiated responses to D1 stimulation (red and orange coded penetrations) in columns surrounding the D1 barrel-column (4/10) in Tx treated mice compared with controls (8/11) shown in **B**. **C)** Vibrissae dominance histograms for the same animals showing the relative response of cells to the spared D1 vibrissa versus their anatomically defined principal vibrissa. The proportion of cells in each bin is plotted where the Vibrissae Dominance Index (VDI) for a given cell is given by VDI = D1/(D1+PW), where D1 is the average response to D1 whisker stimulation and PW the average response to principal whisker stimulation. **D)** Principal whisker responses were not different across Tx treated and vehicle cases ($F_{(1,10)}$=0.12, p=0.91). **E)** The D1 whisker response was 165% greater in mice that had not received Tx at P7 than in DISC1 mice that had ($F_{(1,10)}$=5.68, p<0.05). **F)** The average weighted vibrissae dominance index (see Methods) was also significantly greater for P7 Tx treated animals than controls ($F_{(1,10)}$=16.2, p<0.005).

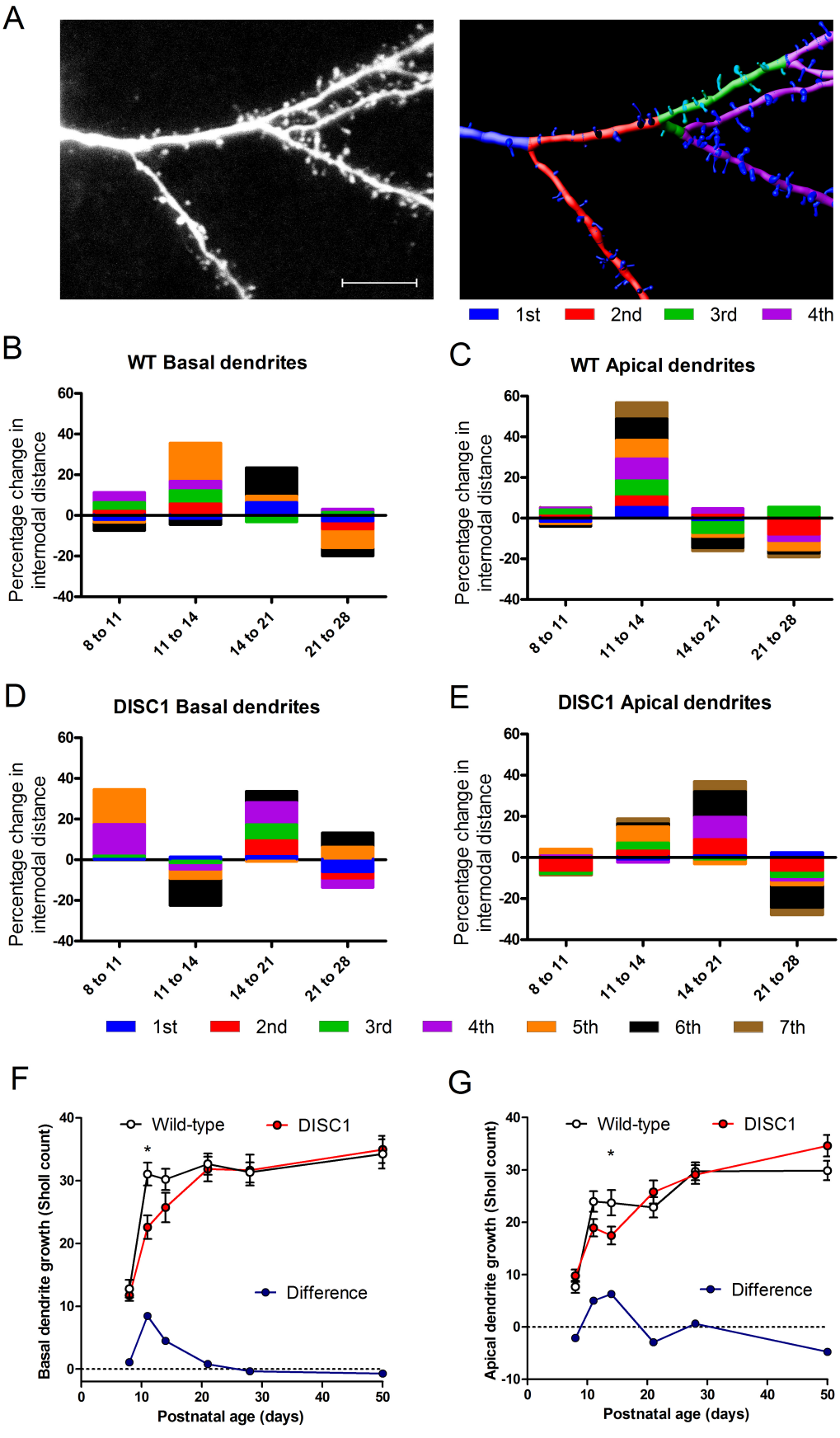

Figure S5. Dendritic development in animals transiently expressing DISC1cc.

A) Example of L2/3 cell dendrites showing spines and dendritic order. Scale bar=10 microns. **B-E)** Growth in dendrites charted as an increase in internodal distances. The change in median internodal distance is given as percentage of the internodal distance at the start of the period. **B)** Wild-type basal dendrites: the main periods of elongation are between 11 and 21 days. Negative values are due to increased branching in that order of dendrite (P21-28). **C)** Wild-type apical dendrites: Almost all the elongation occurs between P11 and 14. **D)** DISC1 basal dendrites: Development of the basal dendrites show a different timecourse to the wild-types. Growth of the 2^{nd} and 3^{rd} order dendrites (red and green) is delayed until P14-21. **E)** DISC1 apical dendrites: Note that 2^{nd} and 3^{rd} order dendrites mainly elongate between P14 and P21 whereas in wild-types the dendrites elongate earlier (P11-14, C). **F)** A plot of basal dendritic growth versus age group shows rapid development between P8 and P11 in wild types (black line white circle). In comparison, the DISC1 dendritic growth (red line) is retarded at P11 and P14 (blue line shows difference in means) and significantly different at P11 ($t_{(40)=}3.23$, $p<0.005$). **G)** The apical dendritic development of layer 2/3 cells is again retarded at P11 and P14 and is significantly different from the wild-types at P14 ($t_{(40)=}2.12$, $p<0.05$).

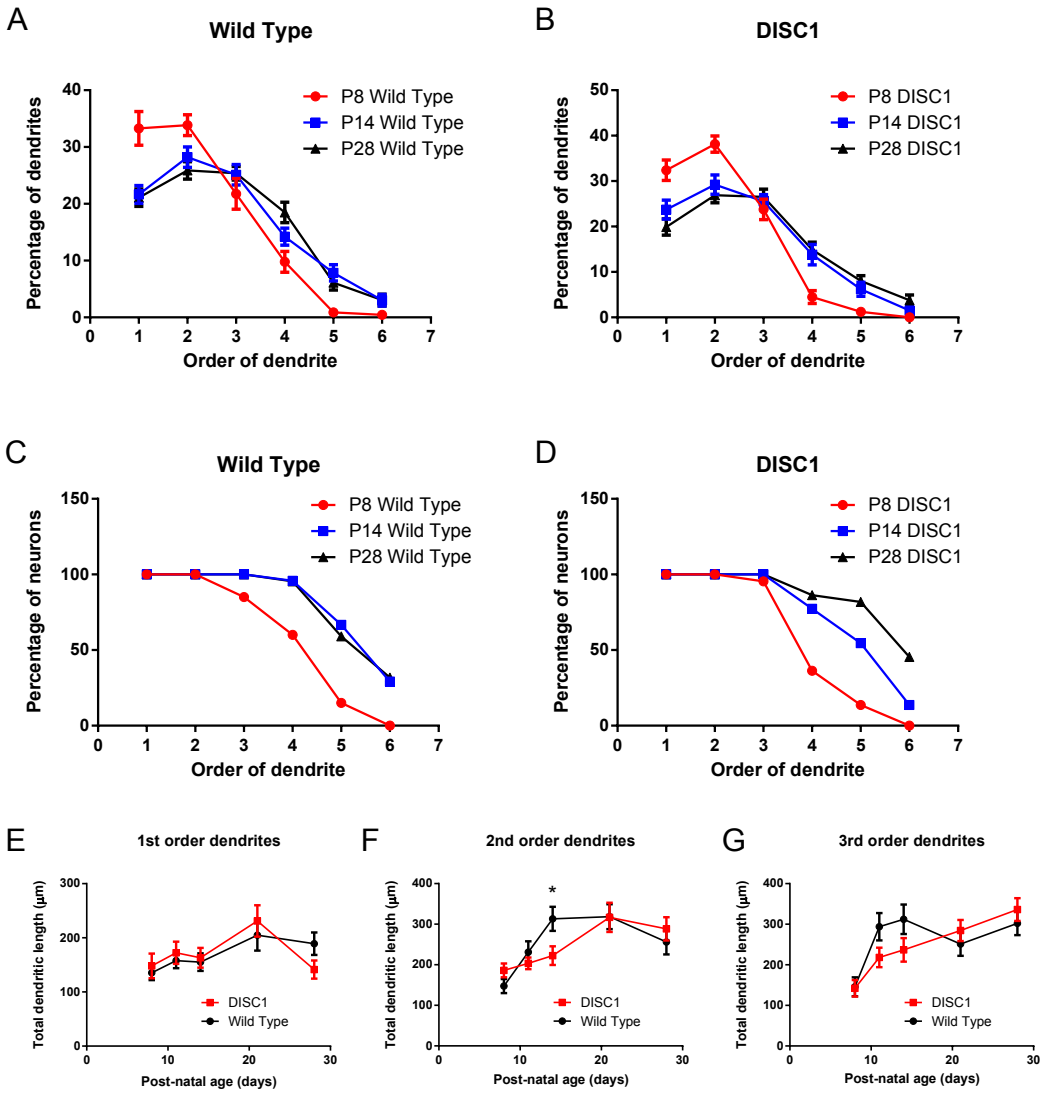

Figure S6. Development of basal dendrites in animals transiently expressing DISC1cc.

A) Wild-type L2/3 neurons: The number of each order of dendrite present at P8 to P28 is expressed as a percentage of the total number of dendritic branches at that age. **B)** The same data as in (A) for DISC1 neurons, showing very similar proportions of each dendrite order between DISC1 and WT animals. **C)** The percentage of neurons possessing each order of dendrite in wild-types **D)** The same form as in (C) plotted for DISC1 mice. **E-G)** The development of dendritic length for each order of dendrite in DISC1 (red) and Wild-type (black) animals. Note that the growth rate in DISC1cc cells is delayed in the 2nd and 3rd order dendrites and significantly smaller at P14 for the 2nd order dendrites (F) ($t_{(42)=}$2.39, $p<0.05$).

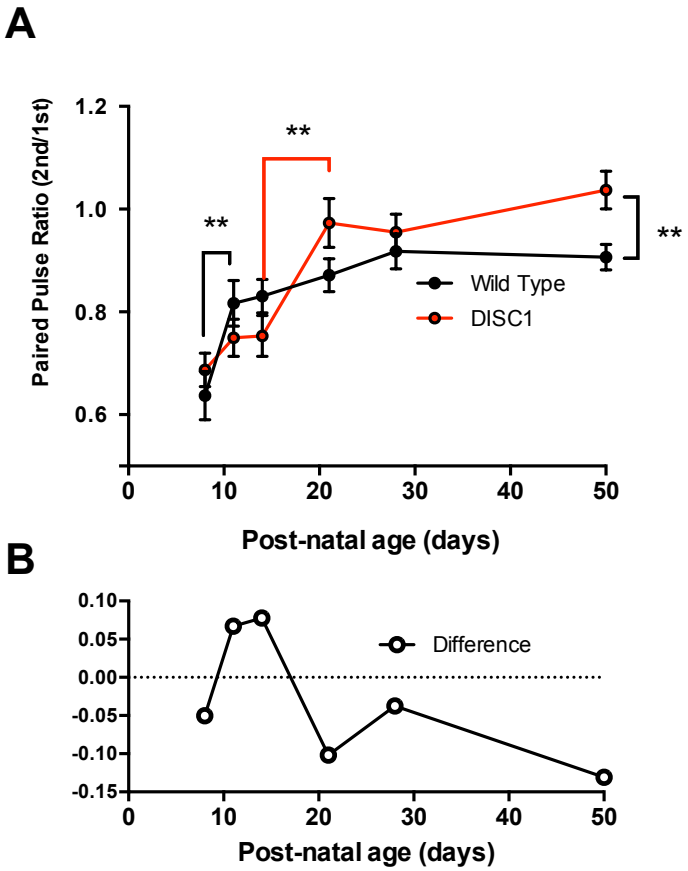

Figure S7. Paired pulse ratio development is delayed by transient release of DISC1cc.

A) The developmental increase in paired pulse ratio is delayed in DISC1cc mice (interaction between age and genotype $F_{(5,5)}$=2.59, p<0.03). In WT mice, paired pulse ratio increases close to adult values between P8 and P11 ($t_{(41)}$=2.76, p<0.01), whereas in DISC1 mice the increase is delayed and occurs between P14 and 21 ($t_{(41)}$=3.46, p<0.005). Adult values of paired pulse ratio are higher in DISC1 mice at P50 ($t_{(46)}$=2.78, p<0.01). **B)** The delay in development and subsequent overshoot can be clearly seen when the difference in paired pulse ratio between WT and DISCcc animals is plotted.

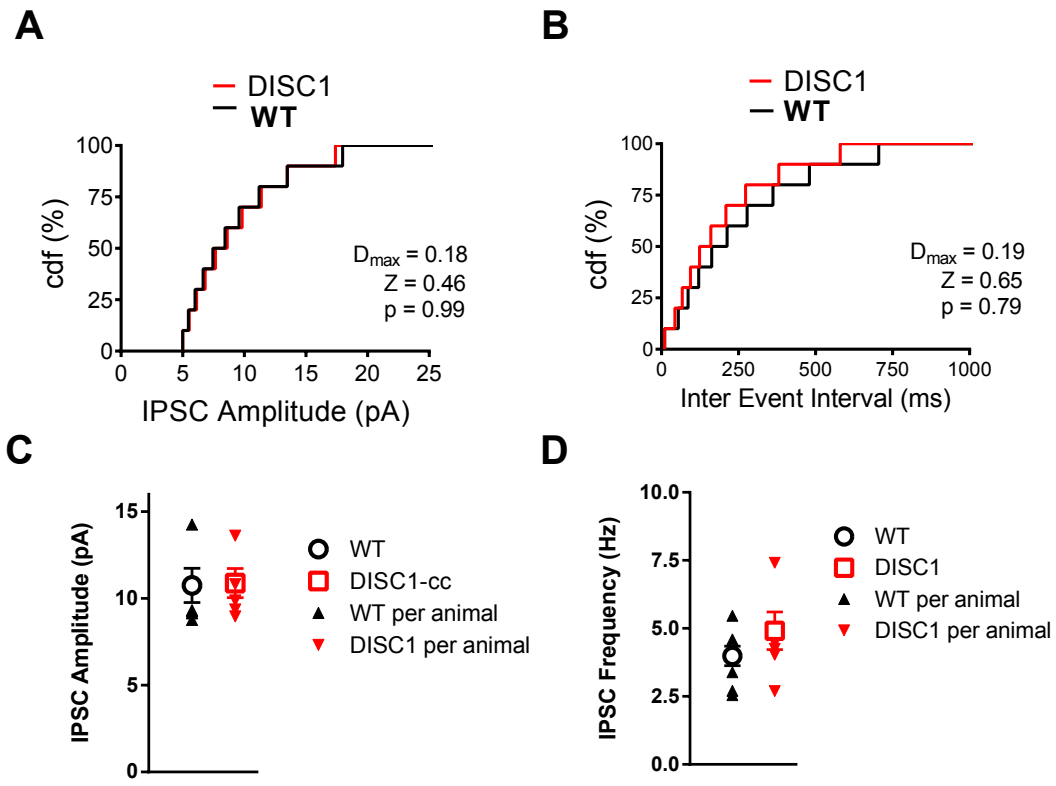

Figure S8. Transient DISC1cc release does not significantly affect inhibitory activity in the barrel cortex.

A) IPSC amplitudes from WT and DISC1 mice were not different to one another (KS test, D_{max}=0.18, Z=0.46, p>0.05) **B)** IPSC inter-event intervals from WT and DISC1 mice were not different to one another (KS test, D_{max}=0.19, Z=0.65, p>0.05). **C)** Mean IPSC amplitudes for WT and DISC1 mice grouped by animal (triangles) and overall mean values (open symbols; WT = 10.76 ± 0.99, DISC1 = 10.89 ± 0.85, $t_{(23)}$=0.11, p>0.05, grouped by animal $t_{(8)}$=0.29, p>0.05). **D)** Mean IPSC frequencies for WT and DISC1 mice grouped by animal (triangles) and overall mean values (open symbols; WT = 3.99 ± 0.36, DISC1 = 4.91 ± 0.69, $t_{(23)}$=1.18, p>0.05, grouped by animal $t_{(8)}$=0.87, p>0.05).

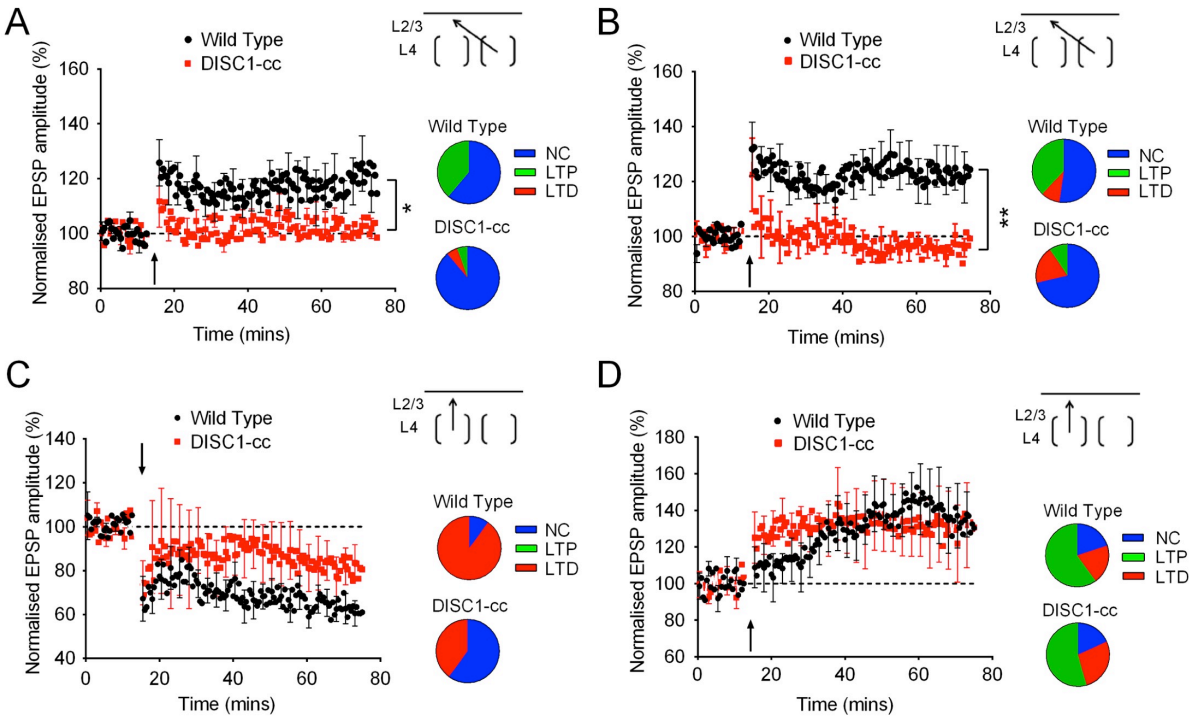

Figure S9. LTP and LTD but not deprivation-unmasked potentiation is impaired in adults by transient DISC1cc release at P7.

A) Transient release of DISC1cc at P7 abolishes the capability for inter-columnar LTP in layer 2/3 at P28 and **B)** at P50 (effect of genotype $F_{(1,74)}$=14.27, p<0.0003, not age $F_{(1,74)}$=0.13, p<0.71, ANOVA). The percentage of cells showing statistically significant LTP drops from 33% in wild-types to 5% in DISC1 (P28) and 43% in wild-types to 9% in DISC1cc at P50 (see pie charts, NC = no change). **C)** Average LTD values are not statistically different in WT and DISC1cc mice ($F_{(1,18)}$=3.44, p<0.08, ANOVA), though the percentage of cells showing LTD drops from 90% in wild-types to 40% in DISC1. **D)** Complete whisker deprivation unmasks PKA dependent loss of depression(20) and this is unaffected in the adult mouse by P7 DISC1cc ($F_{(1,18)}$=0.16, p<0.87, ANOVA).

References

36. X. Li, S. Glazewski, X. Lin, R. Elde, K. Fox, Effect of vibrissae deprivation on follicle innervation, neuropeptide synthesis in the trigeminal ganglion, and S1 barrel cortex plasticity. J Comp Neurol 357, 465 (Jul 3, 1995).

37. M. Armstrong-James, K. Fox, Evidence for a specific role for cortical NMDA receptors in slow-wave sleep. Brain research 451, 189 (Jun 7, 1988).

38. K. Fox, M. Armstrong-James, J. Millar, The electrical characteristics of carbon fibre microelectrodes. Journal of neuroscience methods 3, 37 (Oct, 1980).

39. R. N. Strominger, T. A. Woolsey, Templates for locating the whisker area in fresh flattened mouse and rat cortex. Journal of neuroscience methods 22, 113 (Dec, 1987).

40. M. Wong-Riley, Changes in the visual system of monocularly sutured or enucleated cats demonstrable with cytochrome oxidase histochemistry. Brain research 171, 11 (Jul 27, 1979).

41. N. R. Hardingham, T. Gould, K. Fox, Anatomical and sensory experiential determinants of synaptic plasticity in layer 2/3 pyramidal neurons of mouse barrel cortex. J Comp Neurol 519, 2090 (Aug 1, 2011).

42. D. Feldmeyer, V. Egger, J. Lubke, B. Sakmann, Reliable synaptic connections between pairs of excitatory layer 4 neurones within a single 'barrel' of developing rat somatosensory cortex. The Journal of physiology 521 Pt 1, 169 (Nov 15, 1999).

43. C. W. Bird et al., Moderate prenatal alcohol exposure enhances GluN2B containing NMDA receptor binding and ifenprodil sensitivity in rat agranular insular cortex. PloS one 10, e0118721 (2015).

44. N. Hajos, Z. Nusser, E. A. Rancz, T. F. Freund, I. Mody, Cell type- and synapse-specific variability in synaptic GABAA receptor occupancy. Eur J Neurosci 12, 810 (Mar, 2000).

45. D. A. Sholl, Dendritic organization in the neurons of the visual and motor cortices of the cat. Journal of anatomy 87, 387 (Oct, 1953).

46. C. Wozny, S. R. Williams, Specificity of synaptic connectivity between layer 1 inhibitory interneurons and layer 2/3 pyramidal neurons in the rat neocortex. Cerebral cortex 21, 1818 (Aug, 2011).